An Appraisal of Multiple NADPH Binding-Site Models Proposed for Cytochrome P450 Reductase, NO Synthase, and Related Diflavin Reductase Systems†

Simon Daff*

School of Chemistry, University of Edinburgh, West Mains Road, Edinburgh EH9 3JJ, U.K.

Received November 14, 2003; Revised Manuscript Received February 10, 2004

ABSTRACT: The diflavin reductases exemplified by mammalian cytochrome P450 reductase catalyze NADPH dehydrogenation and electron transfer to an associated monooxygenase. It has recently been proposed that double occupancy of the NADPH dehydrogenation site inhibits the NADPH to FAD hydride transfer step in this series of enzymes. This has important implications for the mechanism of enzyme turnover. However, the conclusions are drawn from a series of pre-steady-state stopped-flow experiments in which the data analysis and interpretation are flawed. Recent data published for P450−BM3 reductase show a decrease in the rate constant for pre-steady-state flavin oxidation with increasing $NADP^+$ concentration. This is interpreted as evidence of inhibition by multiple substrate binding. A detailed reanalysis shows that the data are in fact consistent with a simple single-binding-site model in which reversible hydride transfer causes the observed effect. Data for the related systems are also discussed.

The mammalian cytochromes P450, nitric oxide synthases (NOS),[1] and several other well characterized enzyme systems are reliant on a source of low-potential electrons derived from NADPH dehydrogenation by diflavin reductases. Microsomal cytochrome P450 reductase (CPR) is typical of these, consisting of an FAD-binding NADPH dehydrogenation domain and a flavodoxin-like FMN-binding electron-transfer domain (*1*). The FAD domain is also related by both structure and function to the plant ferredoxin reductase (FNR) family of enzymes. The nitric oxide synthases contain a reductase domain closely related by sequence, structure, and function to CPR, and in cytochrome P450 BM3 (BM3), a similar domain is fused to a bacterial P450 (in *Bacillus megaterium*) to form a self-contained monooxygenase system. All the diflavin reductases function by catalyzing hydride transfer from NADPH to FAD and successive electron transfers from FAD to FMN to the catalytic center (e.g., P450 heme). The crystal structure of CPR shows that the FAD and FMN are extremely close in space, with a distance of only 4 Å between the isoalaxazine components of the flavins (*2*). It is difficult to envisage effective FMN to heme electron transfer occurring with the enzyme in this conformation, which has led to speculation that the component domains possess significant conformational lability. The FAD domain contains a well-defined ADP binding site; in structures of CPR, NOS FAD domain, and FNR, the ADP substituent of $NADP^+$ and substrate analogues is found to anchor the substrate in position. In none of the structures is the nicotinamide substitituent bound in a catalytically functional conformation. However, the structure of the spinach FNR Y308S mutant by Deng et al. shows the nicotinamide stacked above the FAD isoalloxazine ring such that the FAD N5 is only 3 Å from the hydride donor atom of the nicotinamide (*3*). The Y308 residue appears to act as a barrier to FAD nicotinamide stacking and to formation of the productive charge-transfer complex during catalysis. Analogous FAD-shielding residues are present in the diflavin reductases. In neuronal NOS, movement of F1395 has been implicated as the trigger for large-scale conformational changes, which are an important means of regulation in this enzyme (*4*). NADP/H binding has also been shown to control the conformation of the isolated nNOS reductase domain (*5*). The role of conformational changes in the electron transfer and NADPH dehydrogenation steps of the diflavin reductases is therefore an important part of their overall mechanism of action. Recent reports by Scrutton and co-workers on CPR (*6*−*8*), BM3 (*9*), NOS (*10*), and Fdr (*11*) propose that multiple substrate molecules bind to the enzymes and inhibit the NADPH to FAD hydride transfer process, that is, the primary catalytic event. All other steps dependent on substrate binding or conformation would also be affected by multiple occupancy. Recent data presented for BM3 are reanalyzed here to assess these claims.

EXPERIMENTAL PROCEDURES

Kinetic Model for Reaction of the BM3 FAD Domain with NADPH. The reaction of reduced BM3 FAD domain with $NADP^+$ is most simply represented by the model in Scheme 1. The colorless FAD hydroquinone ($FADH_2$) is converted to the yellow oxidized FAD via the hydride-transfer step. The equilibrium position of the hydride transfer is approximately 50:50 according to the reduction potentials of the FAD/H_2 and NADP/H redox couples, which are both −320 mV at pH 7. Consequently, full oxidation of the FAD will only occur when enough $NADP^+$ is present to pull the equilibrium over to the right by binding to the oxidized

† This work was funded by a Royal Society Fellowship and a project grant from The Wellcome Trust.

* E-mail: Simon.Daff@ed.ac.uk. Tel: +44 (0)131 650 7378.

[1] Abbreviations: BM3, flavocytochrome P450 BM3; CPR, cytochrome P450 reductase; NOS, nitric oxide synthase.

10.1021/bi0360408 CCC: $27.50
Published on Web 03/12/2004

Scheme 1: Oxidation of BM3 FAD Hydroquinone by $NADP^{+a}$

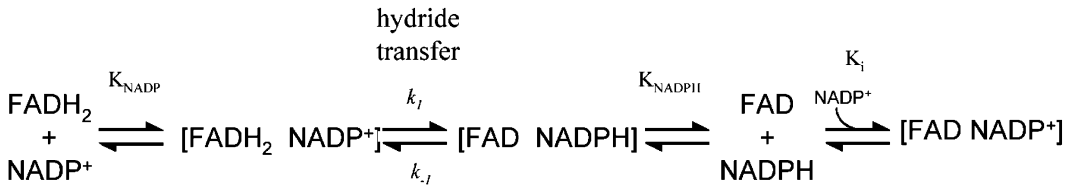

[a] k_1 and k_{-1} are the rate constants for the hydride transfer between $FADH_2$ and $NADP^+$. K_{NADP}, K_{NADPH}, and K_i are the equilibrium constants, as defined in the text.

enzyme and inhibiting the reverse reaction. Strong experimental evidence exists for all the above processes.

In the stopped-flow experiment, the timecourse observed on mixing $FADH_2$ with $NADP^+$ follows the increase in the concentration of oxidized FAD until equilibrium is established. In the simplest case, hydride transfer would be rate-determining in both forward and reverse directions and the timecourse is a single-exponential decay with rate constant equal to the sum of the rates of forward (k_f) and reverse (k_r) hydride transfer at equilibrium.

$$k_{obs} = k_f + k_r$$

In the presence of excess substrate (i.e., [$NADP^+$] > [enzyme]), the dependence of k_f and k_r on substrate concentration is given by standard functions for substrate saturation and competitive inhibition, respectively:

$$k_f = \frac{Nk_1}{N + K_{NADP}} \quad (1)$$

$$k_r = \frac{N_H k_{-1}}{N_H + K_{NADPH}(1 + N/K_i)} \quad (2)$$

where N is the concentration of $NADP^+$ and N_H is the concentration of NADPH. The concentration of NADPH formed at equilibrium can also be estimated from the difference in the reduction potentials for the NADP/H and FAD/H_2 redox couples (ΔE_m) and the total concentration of enzyme (E_t):

$$N_H = N\frac{\sqrt{1 + \frac{4E_t}{N}10^{\Delta E_m/29.5}} - 1}{2 \times 10^{\Delta E_m/29.5}} \quad (3)$$

Combining eqs 1−3 defines the relationship between k_{obs} and $NADP^+$ concentration as plotted in Figure 1. Note that this simple model applies only if the hydride-transfer steps are rate-determining; if either substrate binding or product release were also slow, the reaction time-courses would no longer be single-exponential decays. Further, the equations shown above are applicable only when the concentration of $NADP^+$ is in excess of both the enzyme concentration and K_i, such that pseudo-first order conditions apply to both the forward and reverse reactions. Data fitting was performed using Origin 6.0 (OriginLab Corp.).

RESULTS AND DISCUSSION

Cytochrome P450 BM3. Roitel et al. (*9*) monitored the oxidation of BM3 reductase domain and the isolated BM3 FAD domain by $NADP^+$ using stopped-flow spectrophotometry. In both cases, as the concentration of $NADP^+$ was lowered, the rate constant of the observed exponential decay increased. The failure of the data to fit to a simple Michaelis-type equation led to the proposal that the hydride-transfer process is inhibited by a second substrate molecule binding to the enzyme at high concentrations. However, this analysis does not take account of the fact that when the substrate concentration approaches the enzyme concentration, the Michaelis-type model is no longer valid, that is, in this case the enzyme concentration is 4 μM and the substrate concentration is varied from 2 to 400 μM. In pre-steady-state experiments, the rate of the reverse reaction is of particular importance, because this causes the reaction to reach equilibrium faster. For the BM3 FAD domain, the reduction potential of the $FADH_2$ couple is similar to that of the NADP/H couple (both are −320 mV at pH 7), meaning that the rates of the forward and reverse reactions must be comparable when the product and substrate concentrations are similar. Figure 1 plots the observed exponential decay rate against the $NADP^+$ concentration for the isolated BM3 FAD domain and the C999A mutant (data taken from ref *9*). The FAD domain data set is the easiest to model because only one cofactor (FAD) is involved in the reaction, rather than two in the case of the BM3 reductase domain (FAD and FMN). The oxidation process is represented in Scheme 1 by four consecutive steps, each reversible. These are substrate binding, hydride transfer, product dissociation, and excess substrate binding to the oxidized

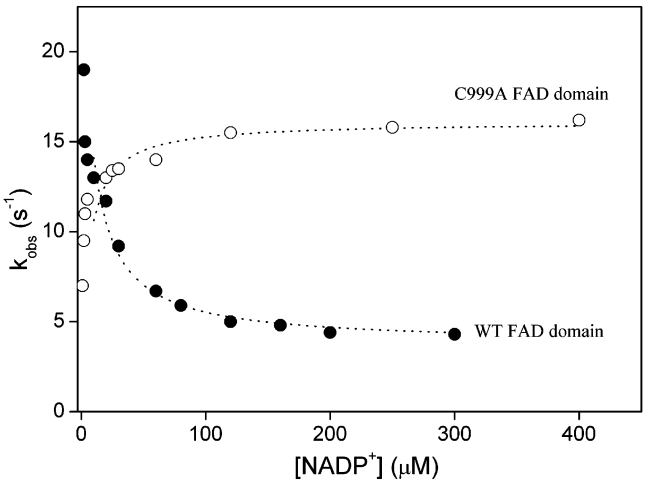

FIGURE 1: Pre-steady-state oxidation of $FADH_2$ by $NADP^+$ in the isolated FAD domains of P450 BM3 and the C999A mutant. The observed rate constant (k_{obs}) determined by fitting stopped-flow absorbance time courses at 450 nm to a single-exponential function is potted against the $NADP^+$ concentration (data obtained from ref 9). The enzyme concentration was 4 μM. The data are shown fitted to the model described by eqs 1−3 with the parameters presented in Table 1.

Table 1: Parameters Describing the Binding and Reaction of NADP(H) with the FAD Domains of P450 BM3 and the C999A Mutant[a]

	BM3 FAD domain	BM3 C999A FAD domain
k_1 (s^{-1})	3.8 ± 1.2	16.1 ± 0.5
k_{-1} (s^{-1})[b]	364[d]	15.9
E_t (μM)[b]	4	4
ΔE_m (mV)[b]	0	−15
K_{NADP} (μM)[c]	5.7[c]	6.3[c]
K_{NADPH} (μM)[b]	22.9[d]	23
K_i (μM)[c]	4.8[c]	3.3[c]

[a] The values were used to model the data presented in Figure 1. The parameters are as described in the kinetic model, eqs 1−3. [b] Values taken from ref 9. [c] Error values obtained for the $NADP^+$ binding constants by least-squares fitting are large due to the close dependency of these parameters. [d] Determined at 5 °C; all other parameters were determined at 25 °C, pH 7.

enzyme. The last step is required for the FAD to be fully oxidized at high concentrations of $NADP^+$ and affects the rate of the reverse process. This is therefore the simplest possible model to adequately represent the reaction. The observed rate of exponential decay is given by combining eqs 1−3. Several of the parameters included in the model were determined by Roitel et al (*9*). These are the enzyme concentration (E_t), the reduction potential of the FAD cofactor, the rate constant for NADPH to FAD hydride transfer (k_{-1}) and the dissociation constant for NADPH from the oxidized enzyme (K_{NADPH}). Unfortunately, the latter two values were only determined from pre-steady-state reduction experiments at 5 °C for the wild-type enzyme; consequently, k_{-1} would probably be 2−3-fold higher at 25 °C.

Iterative fitting was used to determine likely values for k_{-1} ($FADH_2$ to $NADP^+$ hydride transfer), K_{NADP} (the dissociation constant for $NADP^+$ from the reduced enzyme), and K_i (the dissociation constant for $NADP^+$ from the oxidized enzyme). The value calculated for k_1 (Table 1) corresponds to the observed exponential decay rate constant at high concentrations of $NADP^+$ (3.8 s^{-1}). The values calculated for the dissociation constants were very interdependent leading to large errors for these parameters; however, they are not unreasonable (4.8 and 5.7 μM for K_i and K_{NADP}). In fact, Roitel et al. (*9*) determined a K_i value of 7 μM for $NADP^+$ in steady-state cytochrome *c* reduction experiments using the reductase domain, and Murataleev and Feyereisen (*13*) determined the dissociation constant for binding to the reductase domain to be approximately 10 μM using several different methods. The calculated line also appears to fit the experimental data accurately (Figure 1). The value used for k_{-1} in the simulation is likely to be an underestimate, since it was calculated at a lower temperature. Increasing this value has the effect of increasing the rate of the reverse reaction and the observed rate constant at low $NADP^+$ concentrations (i.e., exacerbating the up-turn). This can be compensated for by lower K_{NADP} and K_i values during fitting.

The second data set plotted in Figure 1 is that of the C999A mutant of the BM3 FAD domain, in which a cysteine residue thought to be involved in the hydride-transfer step as a H-bond donor has been replaced by alanine. The mutation has the effect of decreasing the rate of NADPH to FAD hydride transfer dramatically (from 364 to 5 s^{-1} at 5 °C), which lowers the catalytic turnover rate of the enzyme. It also shifts the FAD reduction potential from −320 to −335 mV. These data (Table 1) were incorporated into the model defined by eqs 1−3, and the FAD oxidation rate was simulated as described for the wild-type enzyme. The rate of $FADH_2$ to $NADP^+$ hydride transfer was found to be increased to 16.1 s^{-1} for the mutant, while the dissociation constants K_i and K_{NADPH} were similar to those determined for the wild-type enzyme. The large shifts in the rates of forward and reverse hydride transfer cause the simulation line to invert such that k_{obs} now decreases with the concentration of $NADP^+$, reproducing the trend in the data. In other words, the simple model applies to both wild-type and mutant enzymes equally well, and there is no need to invoke severe structural effects, such as destruction of a substrate binding site, to explain the data.

Overall, the results show that, given a reasonable margin for error in the parameters, both the wild-type and mutant data can be modeled effectively using a simple one-binding-site model. In reality, the substrate binding/dissociation steps are also likely to influence k_{obs} leading to further variables and more possible simulation outcomes. Given the available data, it is impossible to rule out the simple model shown in Scheme 1.

At the present time, there is no evidence to suggest that a second $NADP^+$ binds and inhibits the oxidation process or that the C999 residue stabilizes this species as proposed by Roitel et al (*9*). The simplest kinetic model consistent with the results is the one presented above. However, it is not impossible that alternative binding sites for $NADP^+$ could be mandated by future experiments.

Cytochrome P450 Reductase (CPR) and NO Synthase (NOS). Similar models to that presented for BM3 by Roitel et al. (*9*) were previously used to explain data collected for CPR and NOS by Scrutton, Roberts, and co-workers (*6*−*8*, *10*). In these cases, the observed rate constants for reduction of the enzymes by NADPH increased with decreasing NADPH concentration in stopped-flow experiments. Scheme 1 is reversible, so the model applies equally well in either direction. Unfortunately, the NOS and CPR data sets are not sufficiently accurate or detailed for kinetic modeling, several parameters being unavailable. It is therefore even more apparent that the single-binding-site model cannot be ruled out on the basis of these data, which certainly do not constitute evidence for multiple substrate binding. Further evidence is presented by Gutierrez et al. in the form of stopped-flow premixing experiments using wild-type CPR and the W676H mutant (Figure 7, ref *7*). The mutant reacts more slowly with NADPH due to mutation of the FAD stacking residue (tryptophan) to histidine. On mixing with excess NADPH, the mutant appears to react only partially, indicating that the reaction does not progress to completion. This is interpreted as the reaction of a single equivalent of NADPH at the FAD site followed by the formation of an inhibited complex. Complete reduction (i.e., reduction of both flavins) would require the successive reaction of 2 equiv of NADPH at the FAD site, as observed for the wild-type enzyme. However, premixing with a stoichiometric amount of NADPH and aging for 100 ms followed by reaction with excess NADPH leads to full reduction of the mutant, that is, both NADPH equivalents react. This unusual scenario is explained by a multiple-binding phenomenon, in which an extra molecule of NADPH binds to the enzyme preventing

Scheme 2: Reduction of CPR by NADPH, Including the Proposed Inhibition Complex[a]

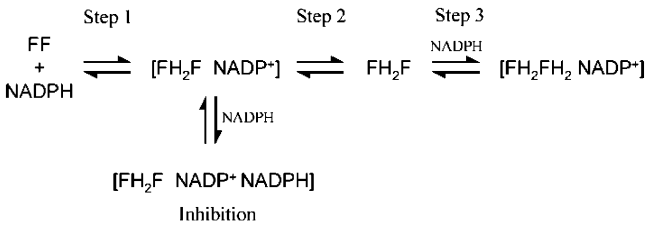

[a] FF is the two flavins (FAD and FMN) of oxidized CPR.

$NADP^+$ release (e.g., Scheme 2), which inhibits the second reduction step. However, Scheme 2 cannot, in fact, explain the observed effect. If step 1 had occurred during the aging process, then one of the two flavins would already have been reduced at the start of the stopped-flow trace. This would have led to less of the reaction being observed than for wild-type CPR, which is not the case. If step 1 had not occurred, then the excess NADPH introduced after aging would result in formation of the inhibited complex. Regardless of its origins, this unusual effect is not observed with wild-type CPR and is an anomaly created by the mutation. Unfortunately, the arguments are based on three single-wavelength stopped-flow traces with no spectroscopic evidence presented for the existence of the inhibited complex. To confirm the assignment, it would have been useful to present the visible spectrum of the partially reduced enzyme existing in the presence of reductant, but this is not shown.

The acceleration of stopped-flow derived rate-constants at substrate concentrations approaching stoichiometry with the enzyme concentration is widely known and has been demonstrated for numerous systems, for example, for FNR with NADPH by Batie and Kamin (*14*). In this case, the kinetics were treated according to Scheme 1 and rate constants were determined with no need to invoke a multiple-occupancy argument.

Simultaneous binding of NADP/H molecules to the ADP and nicotinamide sites of this class of enzymes is made unlikely by the poor affinity of the enzymes for the nicotinamide group. This has been well characterized for CPR by Murateleev and Feyereisen (*12*), who demonstrate that the nicotinamide substituent of $NADP^+$ has a free energy for binding of -0.09 kcal mol^{-1} with the oxidized enzyme, that is, binding is disfavored thermodynamically. Another example is the binding affinity of NAD/H for the enzyme, which is more than 1000-fold lower than that of NADP/H. To cause inhibition over the concentration ranges studied, the molecule binding via its nicotinamide group would be required to have a K_d in the micromolar range.

Certain aspects of the complex hydride- and electron-transfer kinetics exhibited by the diflavin reductases remain to be explained; however, there is no evidence (structural, spectroscopic, or analytical) to suggest that there is a second NADPH binding site in any of the enzymes referred to in this article or that binding via the nicotinamide substituent alone is viable.

ACKNOWLEDGMENT

The author thanks Prof. S. K. Chapman (Edinburgh) for helpful discussions.

REFERENCES

1. Sevrioukova, I. F., and Peterson, J. A. (1995) NADPH-P-450 reductase: structural and functional comparisons of the eukaryotic and prokaryotic isoforms, *Biochemie 78*, 744−751.
2. Wang, M., Roberts, D. L., Paschke, R., Shea, T. M., Masters, B. S. S., and Kim, J. P. (1997) Three-dimensional structure of NADPH-cytochrome P450 reductase: prototype for FMN- and FAD-containing enzymes, *Proc. Natl. Acad. Sci. U.S.A. 94*, 8411−8416.
3. Deng, Z., Aliverti, A., Zanetti, G., Arakaki, A. K., Ottado, J., Orellano, E. G., Calcaterra, N. B., Ceccarelli, E. A., Carrillo, N., and Karplus, P. A. (1999) A productive NADP+ binding mode of ferredoxin-NADP+ reductase revealed by protein engineering and crystallographic studies, *Nat. Struct. Biol. 6*, 847−853.
4. Adak, S., Sharma, M., Meade, A. L., and Stuehr, D. J. (2002) A conserved flavin-shielding residue regulates NO synthase electron transfer and nicotinamide coenzyme specificity, *Proc. Natl. Acad. Sci. U.S.A. 99*, 13516−13521.
5. Craig, D. H., Chapman, S. K., and Daff, S. (2002) Calmodulin activates electron transfer through neuronal nitric-oxide synthase reductase domain by releasing an NADPH-dependent conformational lock, *J. Biol. Chem. 277*, 33987−33994.
6. Gutierrez, A., Grunau, A., Paine, M., Munro, A. W., Wolf. C. R., Roberts, G. C. K., and Scrutton, N. S. (2003) Electron transfer in human cytochrome P450 reductase, *Biochem. Soc. Trans. 31*, 497−501.
7. Gutierrez, A., Doehr, O., Paine, M., Wolf. C. R., Scrutton, N. S., and Roberts, G. C. K. (2000) Trp-676 facilitates nicotinamide coenzyme exchange in the reductive half-reaction of human cytochrome P450 reductase: properties of the soluble W676H and W676A mutant reductases, *Biochemistry 39*, 15990−15999.
8. Gutierrez, A., Lian, L. Y., Wolf, C. R., Scrutton, N. S., and Roberts, G. C. K. (2001) Stopped-flow kinetic studies of flavin reduction in human cytochrome P450 reductase and its component domains, *Biochemistry 40*, 1964−1975.
9. Roitel, O., Scrutton, N. S., and Munro, A. W. (2003) Electron Transfer in Flavocytochrome P450 BM3: Kinetics of Flavin Reduction and Oxidation, the Role of Cysteine 999, and Relationships with Mammalian Cytochrome P450 Reductase, *Biochemistry 42*, 10809−10821.
10. Knight, K., and Scrutton, N. S. (2002) Stopped-flow kinetic studies of electron transfer in the reductase domain of neuronal nitric oxide synthase: reevaluation of the kinetic mechanism reveals new enzyme intermediates and variation with cytochrome P450 reductase, *Biochem. J. 367*, 19−30.
11. McLean, K. J., Scrutton, N. S., and Munro, A. W. (2003) Kinetic, spectroscopic and thermodynamic characterization of the *Mycobacterium tuberculosis* adrenodoxin reductase homologue FprA, *Biochem. J. 372*, 317−327.
12. Murateliev, M. B., and Feyereisen, R. (2000) Interaction of NADP-(H) with Oxidized and Reduced P450 Reductase during Catalysis. Studies with Nucleotide Analogues, *Biochemistry 39*, 5066−5074.
13. Murateliev M. B., and Feyereisen R. (2000) Functional Interactions in Cytochrome P450 BM3. Evidence That NADP(H) Binding Controls Redox Potentials of the Flavin Cofactors, *Biochemistry 39*, 12699−12707.
14. Batie, C. J., and Kamin, H. (1986) Association of ferredoxin-NADP+ reductase with NADP(H). Specificity and oxidation−reduction properties, *J. Biol. Chem. 261*, 11214−11223.

BI0360408